

Hysteresis interaction of radio waves in metals

L M Fisher†, I F Voloshin†, N M Makarov‡ and V A Yampol'skiĭ‡

† All Russian Electrical Engineering Institute, Krasnokazarmennaya Street 12, Moscow 111250, Russia

‡ Institute for Radiophysics and Electronics, Ukrainian Academy of Sciences, Academician Proskura Street 12, Kharkov 310085, Ukraine

Received 16 February 1993, in final form 13 July 1993

Abstract. The interaction of two radio waves with noticeably different frequencies ω and ω_1 ($\omega \gg \omega_1$) inside a tungsten single-crystal plate at liquid-helium temperature have been studied. The magnetodynamic mechanism of non-linearity owing to the existence of the high-frequency wave with a large amplitude \mathcal{H} has been realized. The low-frequency surface impedance \mathcal{Z} was analysed as a function of \mathcal{H} and DC magnetic field H . The hysteresis of $\mathcal{Z}(H)$ was found and studied. The origin of this non-linear phenomenon which has a threshold character is connected with the generation of the current states.

1. Introduction

It is well known that marked non-linear electromagnetic phenomena may be observed in pure metals at low temperatures. Among different origins of such phenomena the magnetodynamic non-linearity is of a specific interest. This non-linearity exists in metals with a large mean free path l of electrons and is connected with the influence of the intrinsic magnetic field of the induced current on the electron trajectories and, therefore, on the metal conductivity. The manifestations of the magnetodynamic mechanism are of great variety (see the reviews in [1–3]). The most important of them are as follows:

- (1) the noticeable deviation in the I – V characteristics of thin metal slabs and wires from Ohm's law in static conditions [4–10];
- (2) the pinch effect and the generation of voltage auto-oscillations at high values of transport current [9, 11];
- (3) the peculiarities of the surface impedance in the case of the non-linear anomalous skin effect [12, 13].

A point that should be mentioned is the current state generation in metals [13, 14]. This specific hysteresis effect of the radio-frequency (RF) current rectification which has no analogy in other media was observed and studied for a number of metals. The theory of current states in metals was developed in [15, 16]. Sometimes, these states are accompanied by low-frequency auto-oscillations and by the occurrence of dissipative electromagnetic structures [17–20].

It should be noted that the energy source of the above-mentioned self-oscillations and dissipative structures is an external high-frequency (HF) electromagnetic wave which excites the current state. This means that there is an interaction between electromagnetic fields of different frequencies. Such an interaction was actually observed in [21]. A sharp increase in the LF surface impedance has been seen within narrow limits of changing the HF wave

amplitude and DC magnetic field. The measurements in [21] were carried out in conditions when hysteresis of the current states does not exist. It is clear that the current state hysteresis must lead to a corresponding hysteresis in the wave interaction too. This paper is devoted just to the investigation of the hysteresis wave interaction onset and to studying the dynamics of its development with increasing wave amplitude.

2. Experiment

The LF surface impedance \mathcal{Z} of a tungsten slab has been measured in a probe field, having a small amplitude $\mathcal{H}_1 = 0.01$ Oe and a small frequency $\omega_1/2\pi = 120$ Hz, as a function of the static magnetic field H parallel to the slab surface. The main aim of our investigation consists in studying the influence of an intense external HF electromagnetic field $\mathcal{H} \cos(\omega t)$ on $\mathcal{Z}(H)$. The vectors of all magnetic fields are collinear. This type of set-up for the experiment arises from the theoretical paper [22] where the non-linear interaction of radio waves in metals was considered.

In [22] the case when the anomalous skin effect conditions are obeyed was studied and the following requirements are met:

$$\omega_1 \ll \omega \ll \nu \quad (1)$$

where ν is the electron relaxation frequency. The spatial distribution of the electromagnetic field inside a metal is characterized by two spatial scales δ and δ_1 representing the anomalous skin depths for both waves. According to (1), these scales are noticeably different:

$$\delta \sim (c^2 l / \sigma_0 \omega)^{1/3} \ll \delta_1 \sim (c^2 l / \sigma_0 \omega_1)^{1/3}. \quad (2)$$

Here σ_0 is the static metal conductivity and c is the speed of light. Naturally, the wave interaction occurs in the interior of the HF skin layer depth δ only where both waves coexist. According to [22], this interaction leads to the appearance of a LF current inside the layer depth δ . Since the depth δ is much smaller than the natural scale δ_1 of LF field change, this current may be considered as a surface type. Thus, owing to the wave interaction, the new unusual scale δ occurs in the LF field distribution.

An analogous surface current appears in the case of the current state generation when HF current rectification takes place in the presence of a DC magnetic field H [23] (see also section 3). The rectified current flowing inside the skin layer depth δ gives rise to a sharp change in the static magnetic field in this region. So, the static magnetic field contains two terms $H + h$ in the sample bulk. The additional term h created by the surface current depends strongly on the fields H and \mathcal{H} : $h = h(H, \mathcal{H})$. In our two-wave case the role of H is played by the field $H + \mathcal{H}_1 \cos(\omega_1 t)$ which changes slowly with time. This means that the expression for the total magnetic field $H_t(x > \delta)$ in a slab outside the skin layer depth δ may be written in the form [22]

$$\begin{aligned} H_t &= H + \mathcal{H}_1 \cos \omega_1 t + h(H + \mathcal{H}_1 \cos(\omega_1 t), \mathcal{H}) \\ &\simeq H + h(H, \mathcal{H}) + (1 + \partial h / \partial H) \mathcal{H}_1 \cos(\omega_1 t). \end{aligned} \quad (3)$$

According to this formula, the amplitude of the LF magnetic field contains an extra factor $\Phi(H, \mathcal{H})$ given by

$$\Phi(H, \mathcal{H}) = (1 + \partial h / \partial H) \quad (4)$$

owing to the wave interaction. The same factor arises in the expression for the LF surface impedance Z [22]:

$$Z(H, \mathcal{H}) = Z(H + h, 0)\Phi(H, \mathcal{H}).$$

The role of this factor is highly essential and may be observed in the experiment. The derivative $\partial h/\partial H$ proves to be much higher than unity if generation of the current state takes place. So, we chose the experimental parameters in such a way that generation of the current state was realized. Our tungsten slabs with a thickness of about 1 mm are characterized by the residual resistance ratio $\rho(300 \text{ K})/\rho(4.2 \text{ K}) \simeq 10^5$ which corresponds to an electron free path of about 1 mm at the temperature $T = 4.2 \text{ K}$. We have measured the surface impedance by the traditional method. The pick-up coil was wound closely on a slab placed into the magnetic field $H + \mathcal{H} \cos(\omega t) + \mathcal{H}_1 \cos(\omega_1 t)$. The pick-up coil signal connected with the response of a slab in an AC external field contains full information about the wave interaction. Using a lock-in amplifier, we extracted the signals proportional to the real part \mathcal{R} and the imaginary part \mathcal{X} of the surface impedance Z . To measure the impedance at low values of H we have compensated for the earth's magnetic field. Furthermore, we could rotate the slab to orient the metal surface parallel to the DC magnetic field H precisely. To justify the orientation of H along the surface we used the strong sensitivity of the RF size effect to the direction of the magnetic field. The amplitudes and frequencies of the HF magnetic field were in the intervals 0–200 Oe and 20–500 kHz, respectively. A static magnetic field was created using a superconducting solenoid.

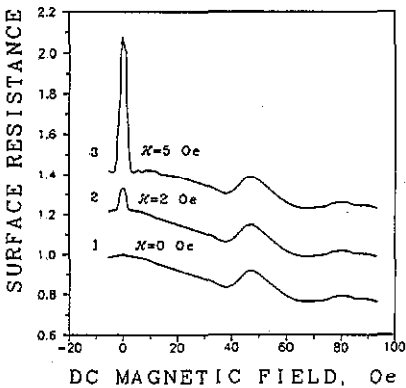


Figure 1. The dependences of the surface resistance $\mathcal{R}(H, \mathcal{H})/\mathcal{R}(0, 0)$ of a tungsten slab with a thickness of 0.9 mm ($n \parallel [100]$) on the DC magnetic field at different amplitudes of the HF wave of frequency $\omega/2\pi = 110 \text{ kHz}$: curve 1, $\mathcal{H} = 0$; curve 2, $\mathcal{H} = 2 \text{ Oe}$; curve 3, $\mathcal{H} = 5 \text{ Oe}$. The amplitude and the frequency of LF field are equal to 0.01 Oe and 130 Hz, respectively. Curves 2 and 3 are shifted along the vertical axis.

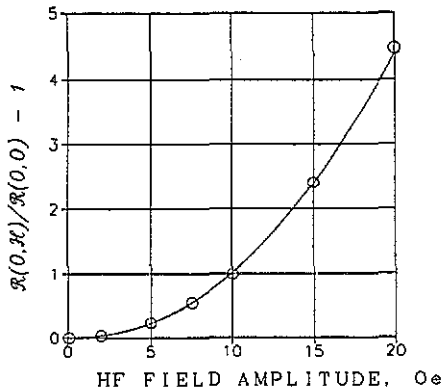


Figure 2. The dependence of $\mathcal{R}(0, \mathcal{H})/\mathcal{R}(0, 0)$ on \mathcal{H} (O) measured under the conditions indicated in the caption to figure 1: —, result of calculations of $\Phi(\mathcal{H})$ using equation (6).

Figure 1 shows the strong influence of the HF wave on the surface resistance of a tungsten slab in the vicinity of $H = 0$. It is clearly seen that the HF wave with even a low

amplitude changes the form of $\mathcal{R}(H)$ qualitatively. Curve 1 obtained in the linear regime has a smooth maximum at $H = 0$. The additional peculiarities for an H of about 40 Oe are connected with the RF size effect. As the amplitude \mathcal{H} of a HF wave increases, a sharp peak arises on the background of a smooth maximum (curves 2 and 3). The amplitude of the peak value $\mathcal{R}(0)$ grows rapidly with increasing \mathcal{H} . The dependence of the peak amplitude on \mathcal{H} is shown as open circles in figure 2. We draw the reader's attention to the great sensitivity of the impedance to the presence of an HF wave. The impedance changes several times owing to the strong wave interaction. These results are in good agreement with the data in [21].

It has been proved that the dependence $\mathcal{R}(H)$ in the linear regime may have another form in the case of thick slabs. This dependence obtained for the slab having a 2 mm thickness is presented as curve 1 in figure 3. Unlike the case of a thin slab the linear surface resistance has a minimum at $H = 0$. Let us consider the impedance change in the non-linear regime in the case of a one-wave situation. When the LF wave amplitude \mathcal{H}_1 exceeds some critical value \mathcal{H}_1^* , a sharp maximum appears and its height grows rapidly with increasing \mathcal{H}_1 . The value of \mathcal{H}_1^* falls if the frequency ω_1 of the LF wave increases or the temperature decreases. As an example, increasing ω from 2 kHz to 100 kHz involves a decrease in \mathcal{H}_1^* from 1 to 0.003 Oe.

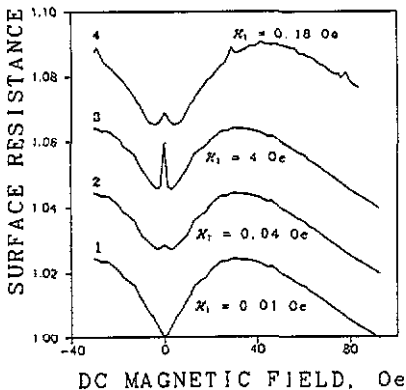


Figure 3. The surface resistance $\mathcal{R}(H)/\mathcal{R}(0)$ of the tungsten slab with a thickness 2 mm as a function of the DC magnetic field at different LF wave amplitudes. The frequency $\omega/2\pi = 21$ kHz, curves 1–3 were obtained at $T = 4.2$ K, and curve 4 was obtained at $T = 1.5$ K, $n \parallel [100]$. Curves 2–4 are shifted along the vertical axis.

The effect of the HF field on the surface impedance becomes more interesting in the region of higher amplitudes of \mathcal{H} . The sequence of curves $\mathcal{R}(H)$ at higher \mathcal{H} is represented in figure 4. The shape of $\mathcal{R}(H)$ changes essentially at some value of \mathcal{H} depending on the frequencies ω and ω_1 . A comparison of the curves in figures 4(a) and (b) shows that the maximum $\mathcal{R}(H)$ bifurcates for an \mathcal{H} of 14 Oe. Moreover, the behaviour of $\mathcal{R}(H)$ becomes irreversible and sharp jumps in the impedance appear at $\mathcal{H} > 15$ Oe. The dynamics of the hysteresis development are illustrated in figure 5. The form of the $\mathcal{R}(H)$ dependence at the highest amplitude $\mathcal{H} = 70$ Oe is presented in figure 6.

3. Discussions

As mentioned above, the nature of the discussed phenomena is connected with the effect of HF current rectification. It is highly essential that equation (5) is valid independent of

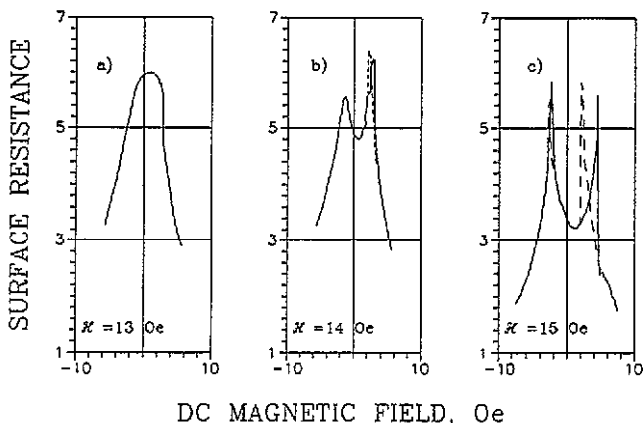


Figure 4. The dependence of the surface resistance $\mathcal{R}(H, \mathcal{H})/\mathcal{R}(0, 0)$ of a slab on the DC magnetic field in the vicinity of the threshold of the current state generation at (a) $\mathcal{H} = 13$ Oe, (b) $\mathcal{H} = 14$ Oe and (c) $\mathcal{H} = 15$ Oe at $\omega/2\pi = 110$ kHz: —, forward magnetic field sweep; - - -, backward magnetic field sweep.

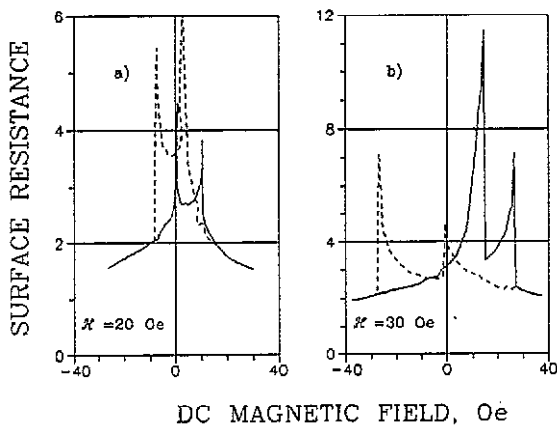


Figure 5. The development of the $\mathcal{R}(H, \mathcal{H})/\mathcal{R}(0, 0)$ hysteresis at high amplitudes of the HF field for (a) $\mathcal{H} = 20$ Oe and (b) $\mathcal{H} = 30$ Oe at $\omega/2\pi = 110$ kHz: —, forward magnetic field sweep; - - -, backward magnetic field sweep.

the real physical origin of this rectification. However, the mechanism of rectification in the conditions of our experiment is well known. It is caused by the current state generation [23]. To understand better the results of our measurements we would like to give a brief picture of this phenomenon. The reason for this effect is connected with the influence of the total magnetic field on the electron trajectories inside the skin layer depth δ . The next figure, 7, adapted from [3], illustrates typical electron trajectories for different moments of the wave period $2\pi/\omega$. When the total magnetic field on the metal surface and the field $H + h$ in the sample bulk outside the skin layer have the same sign, the conductivity of a metal is defined by the group of Larmor electrons. Their trajectories differ very little from Larmor circles in the field $H + h$ (see figure 6(a)). Recall that h is the induced field of the rectified current. In the opposite case, when the total field $H + \mathcal{H}\cos\omega t$ on the metal surface changes its

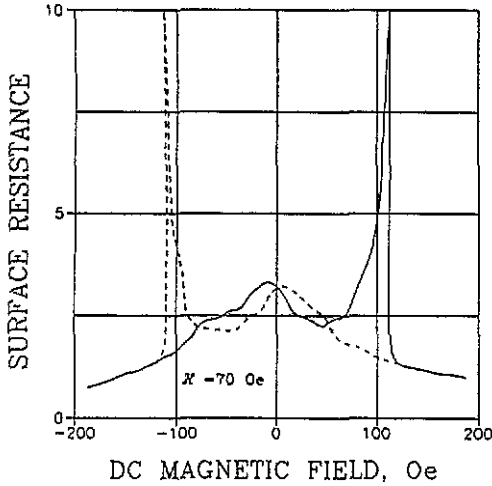


Figure 6. The surface resistance $\mathcal{R}(H, \mathcal{H})/\mathcal{R}(0, 0)$ at $\mathcal{H} = 70$ Oe and $\omega/2\pi = 110$ kHz: —, forward magnetic field sweep; ---, backward magnetic field sweep.

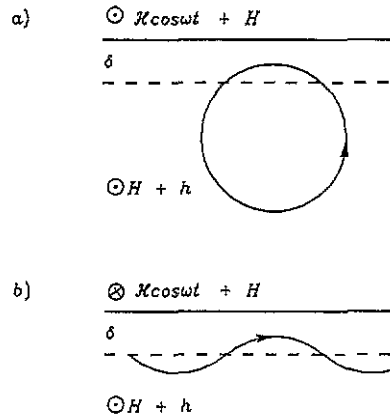


Figure 7. The trajectories of (a) Larmor and (b) twisted electrons (schematic).

sign, a new group of twisted electrons appears (see figure 6(b)). In fact the plane where the total magnetic field changes its sign comes into existence in this case. As a result, the sign of an electron trajectory curvature becomes alternating too. The twisted electrons move inside the skin layer for a much longer time than Larmor electrons and interact with the electromagnetic wave more efficiently. Therefore, the electric conductivity becomes higher during this part of the wave period. Thus, the metal conductivity proves to be a function of time and a rectified current occurs.

The theory of the current states has been given in [15, 16, 23]. The dependence of the induced field h on the amplitude \mathcal{H} and the DC field H was calculated in these papers. According to [16], the function $h(H, \mathcal{H})$ is described by the following expression at low \mathcal{H} :

$$h = (3\sqrt{3}/2\pi)(\mathcal{H}/\bar{h})^2 H \quad \mathcal{H}, H \leq \bar{h} \tag{6}$$

where $\bar{h} = 8cp_F\delta/eI^2$ is the characteristic value of a total magnetic field at which the arc length of the typical electron trajectory equals the electron free path l ; e and p_F are the electron charge and the Fermi momentum, respectively. As we can see from equation (5), the surface impedance has an additional multiplier Φ (4) owing to the wave interaction. This means that the impedance must change quadratically with \mathcal{H} at $\mathcal{H} \leq \bar{h}$. The calculated dependence of $\Phi(\mathcal{H})$ is shown in figure 2 by a full curve. So, the experimental data are in good agreement with the calculated curve.

The curves in figure 8(a) illustrate the dependences of h on H presented in [15] for different values of \mathcal{H} . As the amplitude \mathcal{H} increases, portions with a high derivative $\partial h/\partial H$ appear on the curves $h(H)$. The plots of $\Phi(H)$ for different values of \mathcal{H} are presented in figure 8(b). One can see that Φ has singularities beginning at a critical value of \mathcal{H} , namely \mathcal{H}_c which is little more than \bar{h} . The onset of hysteresis of $\Phi(H)$ occurs at the same value of \mathcal{H} . The theoretical scenario of the hysteresis development shown in figure 8 agrees well with experiment (figures 4–6). First, four hysteresis jumps of $\mathcal{R}(H)$ arise, two of which occur on increasing H and the other two on decreasing H . The first and the second jumps

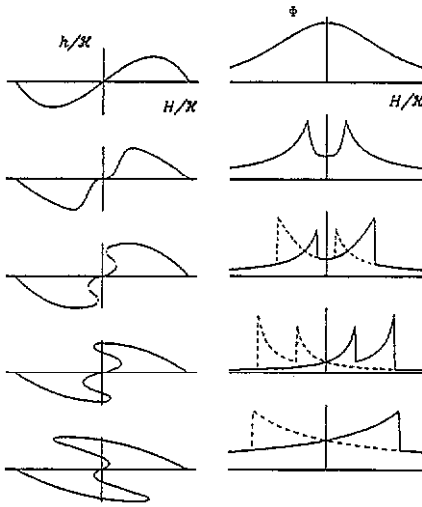


Figure 8. The dependences of (a) h/H and (b) Φ on the DC magnetic field H/H_c (schematic). Beginning from the top of this figure, each subsequent plot corresponds to a higher amplitude of H_c : —, forward magnetic field sweep; ---, backward magnetic field sweep.

of each pair take place at the different signs of H (see figure 5(a) and the third curves from the top in figure 8). As H_c increases, the first pair of jumps displaces to the positive direction of H , whereas the second pair shifts in the opposite direction. Finally beginning from some value of H_c , both jumps of each pair are observed at the same sign of H (see figure 5(b) and the fourth curves from the top in figure 8). The curve in figure 6 obtained at the highest HF amplitude corresponds to the lowest curves in figure 8.

4. Conclusion

Investigation of the wave interaction by measurements of the LF surface impedance is an effective tool for studying the phenomenon of current rectification in metals. In particular, this method permits one to determine precisely the threshold amplitude of H_c for the current state appearance. The high sensitivity of this method is caused by the high value of the derivative $\partial h/\partial H$ in the vicinity of this threshold. The scenario of the critical state development presented above is not unique. Another scenario has been found in [24, 25]. The two-wave method also provides a good possibility for studying this situation too. It should be noted that the current state theory predicts the existence of portions of the curve of $h(H)$ where the factor Φ is negative. This means that the reflected LF wave has a greater amplitude than the incident wave has. To investigate this effect, additional studies are necessary.

References

- [1] Dolgoplov V T 1980 *Usp. Fiz. Nauk* **130** 241 (Engl. Transl. 1980 *Sov. Phys.-Usp.* **23** 134)
- [2] Leviev G I 1988 *Sov. Sci. Rev. A* **11** 103

- [3] Makarov N M and Yampol'skii V A 1991 *Fiz. Nizk. Temp.* **17** 547 (Engl. Transl. 1991 *Sov. J. Low Temp. Phys.* **17** 285)
- [4] Alexandrov B N 1962 *Zh. Eksp. Teor. Fiz.* **43** 1231 (Engl. Transl. 1963 *Sov. Phys.-JETP* **16** 871)
- [5] Yaqub M and Cochran J F 1963 *Phys. Rev. Lett.* **10** 390
- [6] Kaner E A, Makarov N M, Snapiro I B and Yampol'skii V A 1984 *Zh. Eksp. Teor. Fiz.* **87** 2166 (Engl. Transl. 1984 *Sov. Phys.-JETP* **60** 1252)
- [7] Kaner E A, Snapiro I B and Yampol'skii V A 1985 *Fiz. Nizk. Temp.* **11** 477 (Engl. Transl. 1985 *Sov. J. Low Temp. Phys.* **11** 259)
- [8] Voloshin I F, Kravchenko S V, Podlevskikh N A and Fisher L M 1985 *Zh. Eksp. Teor. Fiz.* **89** 233 (Engl. Transl. 1985 *Sov. Phys.-JETP* **62** 132)
- [9] Zakharchenko S I, Kravchenko S V and Fisher L M 1986 *Zh. Eksp. Teor. Fiz.* **91** 660 (Engl. Transl. 1986 *Sov. Phys.-JETP* **64** 390)
- [10] Gaidukov Yu P, Danilova N P and Georgius-Mankarius R Sh 1987 *Zh. Eksp. Teor. Fiz.* **93** 1074 (Engl. Transl. 1987 *Sov. Phys.-JETP* **66** 635)
- [11] Kaner E A, Leonov Yu G, Makarov N M and Yampol'skii V A 1987 *Zh. Eksp. Teor. Fiz.* **93** 2020 (Engl. Transl. 1987 *Sov. Phys.-JETP* **66** 1153)
- [12] L'ubimov O I, Makarov N M and Yampol'skii V A 1983 *Zh. Eksp. Teor. Fiz.* **85** 2159 (Engl. Transl. 1983 *Sov. Phys.-JETP* **58** 1253)
- [13] Voloshin I F, Kravchenko S V, Fisher L M and Yampol'skii V A 1985 *Zh. Eksp. Teor. Fiz.* **88** 1460 (Engl. Transl. 1985 *Sov. Phys.-JETP* **61** 874)
- [14] Dolgoplov V T and Margolin L Ya 1973 *Pis'ma Zh. Eksp. Teor. Fiz.* **17** 233 (Engl. Transl. 1973 *JETP Lett.* **17** 167)
- [15] Makarov N M and Yampol'skii V A 1983 *Zh. Eksp. Teor. Fiz.* **85** 614 (Engl. Transl. 1983 *Sov. Phys.-JETP* **58** 357)
- [16] Makarov N M and Yampol'skii V A 1985 *Fiz. Nizk. Temp.* **11** 482 (Engl. Transl. 1985 *Sov. J. Low Temp. Phys.* **11** 262)
- [17] Babkin G I, Dolgoplov V T and Chuprov P N 1978 *Zh. Eksp. Teor. Fiz.* **75** 1801 (Engl. Transl. 1978 *Sov. Phys.-JETP* **48** 907)
- [18] Voloshin I F, Kravchenko S V and Fisher L M 1986 *Dokl. Akad. Nauk SSSR* **287** 107 (Engl. Transl. 1986 *Sov. Phys. Dokl.* **31** 237)
- [19] Dolgoplov V T and Chuprov P N 1983 *Solid State Commun.* **48** 165
- [20] Kaner E A, Makarov N M, Yurkevich I V and Yampol'skii V A 1987 *Zh. Eksp. Teor. Fiz.* **93** 274 (Engl. Transl. 1987 *Sov. Phys.-JETP* **66** 158)
- [21] Dolgoplov V T, Murzin S S and Chuprov P N 1980 *Zh. Eksp. Teor. Fiz.* **78** 331 (Engl. Transl. 1980 *Sov. Phys.-JETP* **51** 166)
- [22] Makarov N M, Yurkevich I V and Yampol'skii V A 1985 *Zh. Eksp. Teor. Fiz.* **89** 209 (Engl. Transl. 1985 *Sov. Phys.-JETP* **62** 119)
- [23] Babkin G I and Dolgoplov V T 1976 *Solid State Commun.* **18** 713
- [24] Voloshin I F, Kravchenko S V and Fisher L M 1987 *Zh. Eksp. Teor. Fiz.* **92** 1050 (Engl. Transl. 1987 *Sov. Phys.-JETP* **65** 596)
- [25] Makarov N M, Yurkevich I V and Yampol'skii V A 1987 *Fiz. Tverd. Tela* **29** 3349 (Engl. Transl. 1987 *Sov. Phys.-Solid State* **29** 1921)